Proceedings of the 6th International Conference on Biological Engineering and Medical Science
DOI: 10.54254/2753-8818/2026.33015

Dental Cone-Beam Computed Tomography Artifact Mechanisms and Mitigation Strategies

Zhiheng Zhang

School of Radiology, Shandong First Medical University & Shandong Academy of Medical Sciences, Tai'an, China
zhangzhiheng@email.sdfmu.edu.cn

Abstract. Dental cone-beam computed tomography (CBCT) has been a prevalent diagnostic modality in implant planning and endodontic disease because it provides three-dimensional information. However, image quality is often compromised by artifacts, including streaks, bands, shadings and cupping, which result from scatter, beam hardening, photon starvation and metals. These artifacts can reduce contrast, distort gray values, and render fine anatomical details hard to interpret. Artifacts correction strategies are distributed in four steps along the imaging chain: acquisition, projection, reconstruction and post-processing. In general, projection-domain methods are proved to exert the biggest impact, particularly for metal-related artifacts. Additionally, assessment endpoints, CBCT systems and experimental objects varied across studies, making direct comparison of methods difficult. However, each approach demonstrated effectiveness for specific artifact types and imaging conditions. For future methods, powerful functions in spectral CT might be deployed in dental CBCT so that material decomposition and virtual monoenergetic imaging (VMI) can substantially reduce metal artifacts. This review aims to summarize the main artifact types and underlying mechanisms in dental CBCT, as well as evaluating the methods currently used for their mitigation.

Keywords: CBCT, scatter, beam-hardening, photon starvation, metal artifacts.

1. Introduction

Cone-beam computed tomography (CBCT) has become one of the most commonly used three-dimensional imaging modalities in dentistry and maxillofacial practice. Compared with conventional two-dimensional dental radiography, CBCT provides volumetric information and supports multi-planar reconstruction (MPR), which greatly benefits various clinical procedures, such as implant planning, evaluation of complex root canal anatomy, localization of impacted teeth, assessment of jaw lesions, and temporomandibular joint–related imaging. However, CBCT has inherent limitations related to its imaging geometry and data formation. The cone-beam geometry, combined with a large-area flat-panel detector (FPD), typically leads to a higher scatter contribution in the measured projections. As a result, CBCT is more prone to background elevation, reduced contrast, and intensity nonuniformity than idealized imaging models would predict. In addition, patients in oral medicine frequently have high-attenuation structures: dense cortical bone, metallic restorations,

© 2026 The Authors. This is an open access article distributed under the terms of the Creative Commons Attribution License 4.0 (https://creativecommons.org/licenses/by/4.0/).

DOI: 10.54254/2753-8818/2026.33015

orthodontic appliances, and dental implants, which further exacerbate artifact formation. Consequently, artifacts in dental CBCT are the predominant factor which can limit image reliability.

Among the many sources of CBCT image degradation, scattering- and beam hardening-related artifacts, as well as metal-related artifacts driven by high-attenuation materials, are the most typical physics-dominated artifacts in dental imaging. Scattering engenders a spatially varying background signal in the projections, reducing contrast and manifest as cupping artifacts or shading-like nonuniformity after reconstruction. Beam hardening stems from the polychromatic X-ray spectrum, which breaks the assumption that the log-transformed projection equals a line integral of linear attenuation. Lower-energy photons are partially absorbed, resulting in beam hardening that produces cupping artifacts, dark bands, and streaking. When high-attenuation materials like metallic restorations or implants exist, related effects often interact and intermingle, forming stronger streaks and shadows that obscure critical details. These artifacts can wind down diagnostic confidence, mangle lesion boundaries, and compromise subsequent tasks such as threshold-based segmentation, assessment of peri-implant bone integrity, and any quantitative analysis relying on gray-value/CT-number consistency. With dentistry increasingly adopting digital and precision workflows, comprehending and solving physics-driven artifacts is pivotal for more reliable clinical decision-making.

Recent studies suggest that the severity of scattering, beam hardening, and metal-related artifacts in dental CBCT depends jointly on system design, acquisition protocol, and the object. Larger fields of view, larger object sizes, and limited anti-scatter capability generally increase scatter fraction and worsen intensity nonuniformity. Beam hardening becomes more noticeable if dense bone and metallic materials are in presence, producing cupping artifact, dark bands, streaking and shading patterns. Metal-related artifacts render lesions particularly ambiguous near implants and restorations, where strong streaks and shadows might obscure adjacent structures. To mitigate these effects, multiple strategies have been proposed across the imaging workflow. At the acquisition level, susceptibility of producing artifacts dwindles via selecting appropriate fields of view (FOV), exposure parameters, and filtration. These measures are preventive but constrained by device capabilities and clinical practicality, and their impact are unsatisfactory. Approaches in the pre-processing level aim to rectify the data in vicinity of its origin, such as scatter estimation, subtraction, beam-hardening correction, and metal artifact reduction (MAR) procedures. These techniques can be effective but depend on accurate modeling and calibration and may introduce new nonuniformity if assumptions are jeopardized. Reconstruction-level methods including iterative or model-based techniques, aim to incorporate physical process of scattering and beam-hardening into the model, potentially enhancing gray value and CT number consistency and capability of calibration, but they are computationally demanding and harder to deploy. Finally, image-domain methods in post-processing, including traditional filters and data-driven methods such as deep learning, can further suppress residual artifacts after reconstruction and is often easier to integrate, yet it risks losing normal anatomical detail and the introduction of unauthentic structures. In conclusion, despite huge progress, challenges remain in the trade-off between artifact suppression and preservation of fine anatomical details, as well as the lack of standardized evaluation metrics.

In conclusion, despite significant progress, challenges remain in balancing artifact suppression with the preservation of fine anatomical details, and there is a lack of standardized evaluation metrics. This review aims to summarize the physical mechanisms and typical appearances of artifacts in dental CBCT. It also compares mitigation strategies at four stages of the imaging chain, including acquisition, pre-processing, reconstruction, and post-processing. Key research gaps, including evaluation inconsistencies and clinical deployment challenges, are identified. Lastly,

DOI: 10.54254/2753-8818/2026.33015

future research directions, like standardized evaluation methods and task-oriented metrics, are outlined to improve artifact mitigation and clinical outcomes.

2. Artifact mechanisms in dental CBCT

2.1. Scatter-induced artifacts

In dental CBCT, scatter often causes decrease contrast of structures and Hounsfield Units (HU) inaccuracy, sometimes artifacts appeared as shadings and streaks. Zhao et al. explicitly stated the reason is that scatter contaminates the projections therefore violating the reconstruction algorithm [1]. Figure 1 illustrates how scatter disrupts the ideal line-integral model.

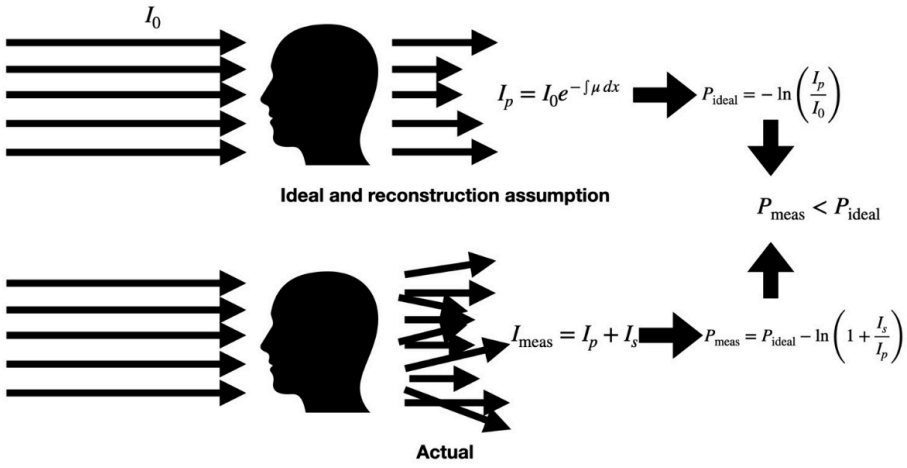


Figure 1. Mechanism of scatter violating line-integral model [1]

The intensity of scatter varies across detector pixels and projection angles, meaning the scatter-to-primary ratio is a variable, different regions of the image receive different amounts of extra X-ray. Linear attenuation coefficients in pixels which reconstruction further calculates are deviated, leading to lower contrast of all structures, general HU inaccuracy, and shadings in low-frequency space and streaks between high-contrast objects might be introduced.

2.2. Beam hardening effects

The polychromatic energy produced by X-ray tube is the only kind of beam energy available currently. Because high-density and high-atomic number objects absorb huge quantity of low-energy photons, the average energy of beam passing through is elevated. Therefore, these beams with stronger penetration ability leave more intensity in the detector pixels, rendering related regions darker in the final image. Sawicki et al. noted that beam-hardening effect is stronger in the central region, which causes the cupping artifact that central gray values are lower than the edges. Additional beam-hardening-related artifacts include dark bands, streaks between multiple metals and pre-implant artifacts. Figure 2 shows that these effects can compromise quantitative measurements and obscure fine anatomical structures [2].

DOI: 10.54254/2753-8818/2026.33015

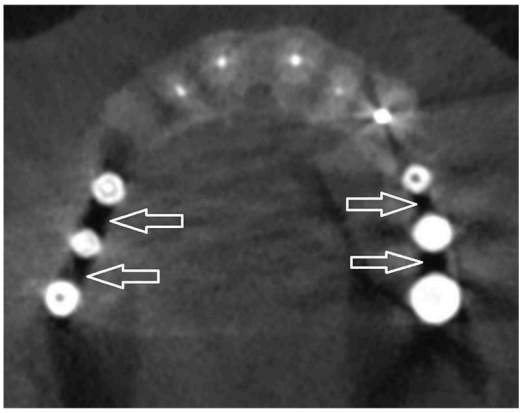


Figure 2. Dark streaks between dental implants in CBCT [2]

2.3. Photon starvation artifact

Photon starvation means that photons arrived at the detector along some beam directions become too few. High-attenuation objects, such as metallic restorations or implants, are considered as the culprit, and this effect can be especially escalated in low-mAs conditions like dental CBCT. A reduced photon count results in increased image noise and graininess. Zeng et al. said that what photon starvation adds to the image are more than just noise, it also involves bright and dark steaks. Owing to too little number of photons, the variance of projection values along the paths where beams are hugely attenuated becomes large, which means signal variation is concentrated in these certain directions. Therefore, bright and dark steaks are reconstructed instead of only uniform noise [3]. Furthermore, Figure 3 shows that photon starvation is a major contributor to pre-implant artifacts together with beam hardening [2].

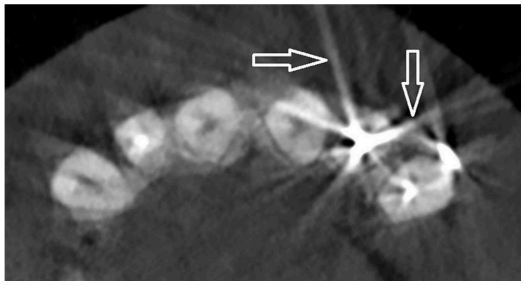


Figure 3. Photon starvation effect generating substantial noise and streaks around metal post and core in the anterior maxillary tooth [2]

2.4. Metal artifacts

The three mentioned above together are viewed as the elementary sources of metal artifacts and metals simply amplify their impacts and give rise to more pronounced streaks and bands [4]. The interaction of these mechanisms produces more pronounced streaks, dark bands, and shading, which can obscure anatomical details and complicate diagnosis. The severity and pattern of these artifacts are influenced by the number, composition, and spatial arrangement of metallic objects. Effective mitigation of metal-related artifacts therefore requires strategies that address all underlying mechanisms rather than single isolated factors.

DOI: 10.54254/2753-8818/2026.33015

3. Methods for artifact reduction

3.1. Acquisition and projection-domain correction

The primary approach to mitigating dental CBCT artifacts focuses on addressing scatter and metal-related effects in the raw data or before reconstruction. A collective character of these methods is not perceiving artifacts as problems after reconstruction. Instead, they aim to enhance the extent that the projection signal matches the true line integral before the data are transferred into FDK or other reconstruction algorithms, which means reducing the contamination to the ideal projection integral model. Derived from the current literature, acquisition and projection-domain approaches mainly focus on three sorts of problems: scatter filtration, correction of projection inconsistencies brought in by metal or beam hardening, and projection-domain detection and correction for metals which are outside the FOV or across boundaries of FOV.

3.1.1. Two-dimensional anti-scatter grid and scatter suppression

Scatter filtration is most hardware-related method in the acquisition of dental CBCT. Li et al. mounted a two-dimensional anti-scatter grid (2D ASG) in a dental CBCT's hardware-equipment and directly rectified the residual scatter in the raw projections via a measurement-based correction method called Grid-based Scatter Sampling (GSS). By performing phantom experiments instead of clinical data, their results demonstrated that about 10 to 20 times of scatter-to-primary ratio (SPR) in CBCT projections were reduced in the ASG + GSS group comparing to the group without ASG and GSS under the same scanning conditions. For the tooth HU nonuniformity aspect, after the hardware system incorporated the ASG and the GSS was deployed, the maximum HU difference among different tooth ROIs dwindled from 510 HU to 146 HU. Comparing to exposure without the grid and projection-domain correction, contrast ascended by 27% in the bone-equivalent region with the 600 mg/mL calcium inserted, increasing from 1345 ± 117 HU to 1782 ± 143 HU [5].

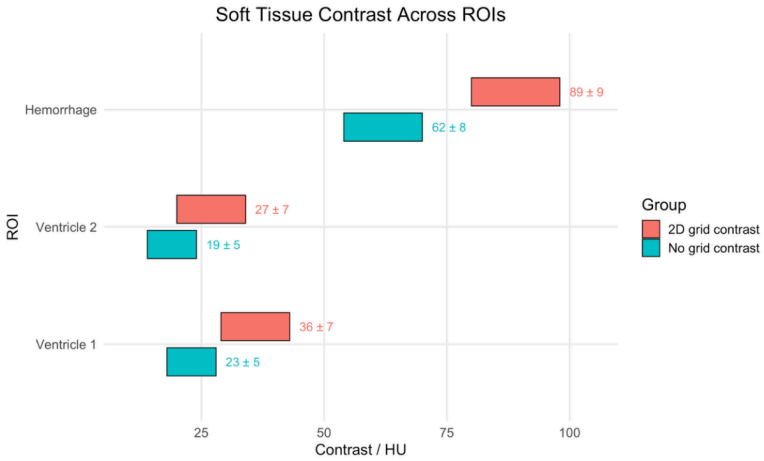


Figure 4. Soft tissue contrast across ventricles and hemorrhage in the phantom [5]

Soft tissue contrast was also elevated by 42.1% to 56.5% in the ROIs where the brain phantoms were equivalent to ventricle, 43.5% in the Hemorrhage-equivalent ROI. At last, in brain soft tissue phantom, the standard deviation of mean HU decreased from 4.8 HU to 2.4 HU. In the skull bone phantom, it decreased from 208 HU to 104 HU. These improvements indicate that the 2D grid not only reduced artifacts, but also significantly optimized the image-quality related metrics (Figure 4).

DOI: 10.54254/2753-8818/2026.33015

However, limitations were acknowledged: (1) the grid prototype is only able to cover about 18% of the FOV in the cranio-caudal direction, which means it is only suitable for small FOV inspections. (2) The image-processing software and 2D-grid implementation currently are not compatible. (3) There were no signs that noise was lessened [5].

Sabounchi et al. aimed to resolve the HU/ tissue density inconsistency problem that clinical dental CBCT often does not represent real tissue density accurately, which usually brings about difficulties in quantitative imaging like 3D reconstruction. Similar to Li et al., their method did not only rely on the 2D ASG hardware to reduce scatter at the acquisition stage. For the small fraction of residual scatter that passed through the 2D ASG and reached the detector, they too adopted an additional measurement-based scatter correction in projection step before reconstruction. What differentiated from Li et al. was that they built an experimental benchtop CBCT equipment which was fully interoperable with the 2D ASG, and produced a 3D-printed phantom, as well as including clinical CBCT and MDCT as comparators.

In this study, for the simulated benchtop dental CBCT, the 2D ASG rendered the median HU non-uniformity in soft tissue-equivalent regions dwindled by 18.7 HU, and 32.1 HU in tooth-equivalent Teflon regions. The grid also enhanced HU stability, mitigating the susceptibility of tooth HU values to variations in FOVs. Also, the 2D ASG reduced the HU loss due to implant-induced streaks for about 40 HU. In addition, median contrast-to-noise ratio (CNR) improvement with the 2D ASG was 37.7% and the FOV dependence of CNR was curtailed owing to the 2D ASG which was more beneficial at larger FOVs. Cross-modalities comparison demonstrated that the benchtop CBCT with 2D ASG produced HU values closer to MDCT and reduced severe streaks compared with clinical dental CBCT. In HU nonuniformity the simulated CBCT with 2D ASG also approached the MDCT more than the clinical CBCT.

This example illustrates that hardware-based scatter suppression can substantially improve projection fidelity and quantitative image metrics in dental CBCT. However, several gaps and drawbacks still persist. Although comprehensive fluctuating factors had been made allowances for, the transverse/axial FOV was kept unaltered, which led to the unawareness of the effect of the 2D ASG in smaller transverse/axial FOV protocols. Additionally, high-frequency marginal and peripheral streaks were not fully eliminated, likely due to the limited number of projections in the experimental CBCT. At last, the enhancement of CNR were inconspicuous in small FOVs when ASG was deployed [6].

3.1.2. Direct Sinogram Correction and metal path-length weighting

An existing projection-domain method, Direct Sinogram Correction (DSC) which rectifies projection data so that the data are more aligned with the Radon transform assumption (a prerequisite for FBP), was proved to be insufficient when multiple metallic objects are present or beam-hardening artifacts are substantial. In a representative patient case, Hegazy et al. pinpointed that the mean projection intensity on a non-overlapped metal trace was 5.75, while the counterpart value on a 3 metal-overlapped trace was 4.62. This discrepancy contradicted the physical anticipation that longer metal paths should produce higher projection values, which suggested that the original DSC under-corrected heavily attenuated metal paths. In order to refine DSC, Hegazy et al. embedded the metal path-length weighting that can render stronger correction administrated to X-rays passing through more metals. The method was evaluated using both a contrast-agent phantom and clinical dental CBCT data.

DOI: 10.54254/2753-8818/2026.33015

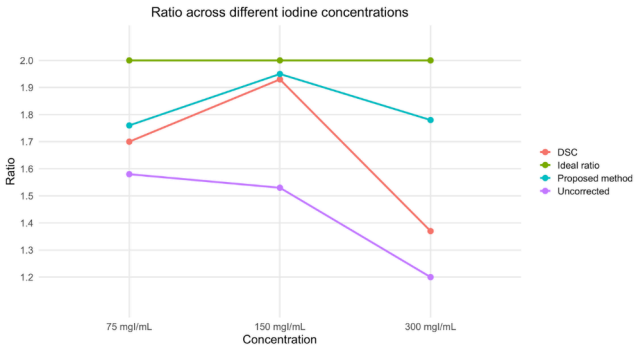


Figure 5. The intensity ratio for different iodine concentration and different methods [7]

The quantitative metric in phantom was that the ratio of average signal in a metal-overlapping region versus a non-overlapping region in the sinogram of 3 groups which corresponded to 3 different iodine concentrations: 300 mgI/ml, 150 mgI/ml, 75 mgI/ml. As shown in Figure 5, the ratio of average signal in metal-overlapping and non-overlapping regions improved after correction, particularly with the proposed method. This ratio should reach 2 in an ideal model. Before any correction, these values were 1.20, 1.53, and 1.58. After applying DSC, they reached 1.37, 1.93, and 1.70. After using the proposed method, the ratios further improved to 1.78, 1.95, and 1.76. The point which warranted biggest attention was that 300 mgI/mL rose from 1.37 with DSC to 1.78 with the proposed method. As well as the acrylic structure was still quite invisible in DSC-corrected image but became clearly visible after employing the metal path-length weighting, indicating that this method was dedicated for most severe artifacts area where DSC often plays a minor role. Clinical images included multiple patients with variable implant positions, numbers of crowns and fillings, and distances between materials. Across all cases, qualitative observation suggested that the proposed method performed better than uncorrected and DSC-corrected ones in terms of streaks, dark bands, long shadings and manifestation of lesion details.

As for the limitations of this method, first, this modification of DSC lacks proper and rigorous mathematical deduction and verification, which means it is only empirical-supported. Second, in the qualitative evaluation of patient images, no artifact-free CT image was available as a ground truth, and a panoramic image was used as an aid, which may limit the robustness and accuracy of subjective assessments [7].

3.1.3. Projection-domain metal detection using a dual-layer detector

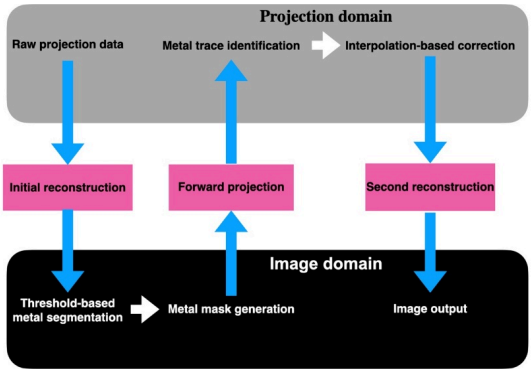


Figure 6. The workflow of the two-pass method [8]

DOI: 10.54254/2753-8818/2026.33015

The workflow of traditional two-pass method is illustrated in Figure 6. A key limitation of this image-based modality is that it loses effectiveness if metals cannot be detected in the initial reconstructed image, which causes failures in subsequent steps. Cases that metals located outside the FOV or across the edge are present and metals move during the scan entail a new strategy. Therefore, Shi et al. proposed a single-pass projection-domain modality combined with a dual-layer flat-panel detector (FPD) in order to bypass the first direct reconstruction step. The workflow of single-pass method is illustrated in Figure 7.

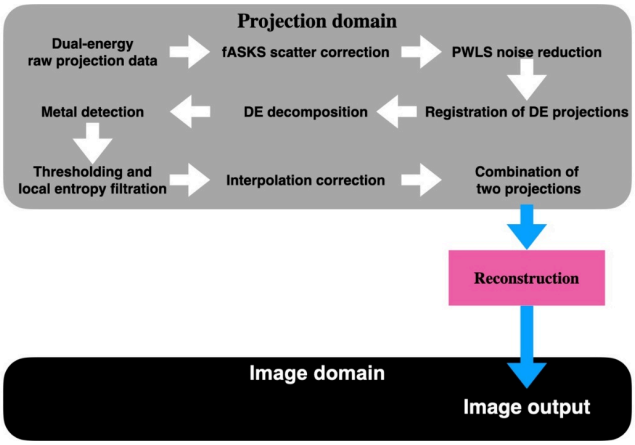


Figure 7. The workflow of the single-pass method [8]

This approach uses a dual-energy and dual-layer FPD to scan a liver biopsy phantom and a cadaver head separately. Comparisons were made between the single-pass projection-domain method and the two-pass image-domain method, single-layer (SL) versus dual-layer (DL) detectors, and Markov random field (MRF) versus thresholding approaches. The quantitative results in the liver phantom are shown in Figure 8, and soft-tissue standard deviation in the cadaver head is illustrated in Figure 9.

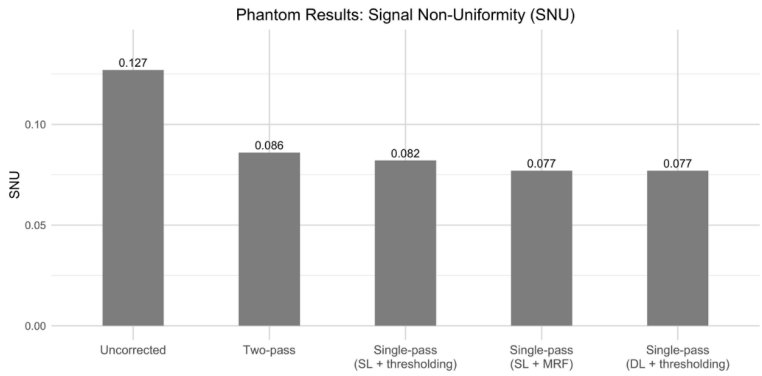


Figure 8. The signal non-uniformity (SNU) in the liver biopsy phantom [8]

DOI: 10.54254/2753-8818/2026.33015

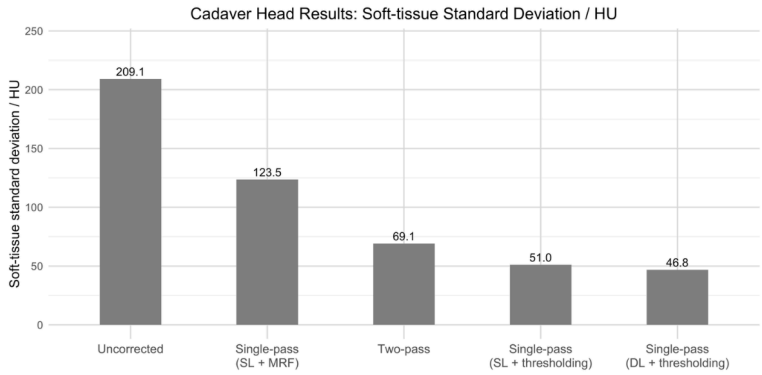


Figure 9. The soft-tissue standard deviation in the cadaver head [8]

From the statistics above, the single-pass projection-domain method (DL + thresholding) decreased SNU in the liver phantom from 0.086 to 0.077 compared with the two-pass image-domain method, achieving a 43.5% additional reduction in artifacts. In the cadaver head, 22.3 HU in soft-tissue standard deviation was further dwindled owing to supplanting the conventional method with the proposed one, from 69.1 HU to 46.8 HU, and 32.2% enhancement in HU uniformity was accomplished by this method. In addition, single-layer detectors produced more false positives in both thresholding and MRF, whereas dual-layer detectors enhanced the visibility of metals against the background. For the time efficiency aspect, 31% processing time was shortened by proposed method in comparison with the conventional one.

However, some limitations in the new method must not be ignored. First, new streaks may be created due to the interpolation especially when heterogeneous structures overlaps. Second, a trade-off that Detective Quantum Efficiency (DQE) will be sacrificed in compensation for better spectral separation is something needed future optimization [8].

3.2. Iterative reconstruction for improved robustness

Differentiated from projection-domain methods, reconstruction-stage methods do not aim to directly rebuild more correct projections. Instead, they improve image quality through a more robust reconstruction model. As we know, a classic feature of dental CBCT is its relatively low energy X-ray beam which introduces more noise and more beam-hardening artifacts. To determine whether iterative reconstruction (IR) performs better than filtered back projection (FBP) in terms of noise and artifact reduction, Ramage et al. used a dental CBCT unit that allowed free switching between standard FBP and IR modes, with optional application of metal artifact reduction (MAR). Scans were performed on a human dentate mandible phantom before and after the placement of a titanium implant under varying FOVs, acquisition modes, tube current (mA) and MAR settings.

The major finding and the most significant result in statistic was that the general mean noise was 198.65 ± 55.58 for FBP and 99.84 ± 16.28 for IR, which indicated approximately 49.7% noise was reduced. Also, the noise-reducing ability of IR manifested little susceptibility to whether the metal implant was embedded. Relative to FBP, the average noise reduction of IR only fluctuated about 5%. The results across different FOVs, acquisition mode and mA suggested that IR showed superiority in noise reduction over FBP in situation where FOV was large, acquisition mode was switch to low dose and mA was also low. For comparison with and without the MAR, the fluctuation of this metric was only about 5%, meaning the compatibility with MAR was acceptable. In terms of

DOI: 10.54254/2753-8818/2026.33015

processing time difference, the mean additional time that IR added was 35.1 s across all those scans, falling in the scope from 21 to 49 s.

A reconstruction method unique to a specific CBCT unit is difficult to implement on other systems that do not incorporate the same algorithm. Therefore, IR has been proved better than FBP only for the specific dental CBCT in this study, so its practicality entails further investigation. Second, although the additional processing time was of little consequence via IR in this study, a dedicated GPU was required for computation, indicating that iterative reconstruction is highly computationally demanding [9].

3.3. Image-domain post-processing and deep learning

3.3.1. A hybrid model of latent diffusion and modified Normalized Metal Artifact Reduction

The classic Normalized Metal Artifact Reduction (NMAR) has always been debated for its critical flaw: heavy dependence of the prior image. Meanwhile, the traditional Deep Learning has not been fully refined. Currently, it obscures real anatomy structures and details which has been prioritized in oral medicine. To address these challenges, a hybrid approach combining a Latent Diffusion Model (LDM) with a modified NMAR was developed to mitigate dark bands and streaks while preserving anatomical details. The complete workflow is illustrated in Figure 10.

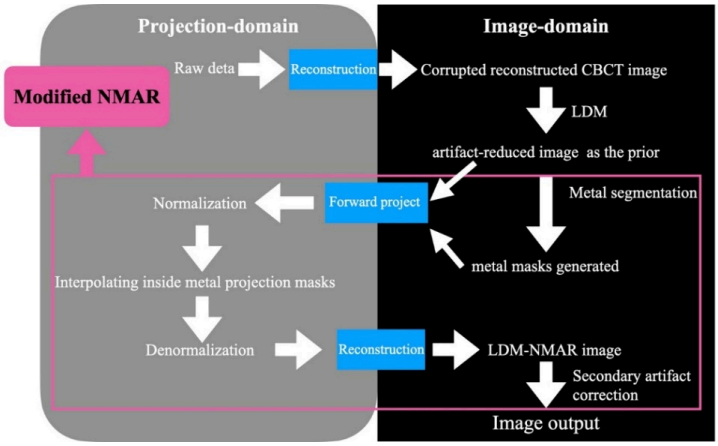


Figure 10. The workflow of LDM-NMAR [10]

In this method, the first reconstructed image without any MAR was used by LDM as the condition to preserve anatomy details. The LDM was to provide a better prior image for NMAR, but still with blurring structures existing. Steps 4 to 9 involve locating metals, forward projecting the metal mask and LDM prior, and applying NMAR in the projection domain. A secondary correction is applied using an interpolation algorithm, normalized to facilitate accurate pixel correction, to compensate for artifacts introduced during interpolation. The method was evaluated on both phantom and clinical CBCT datasets, with comparators including conventional NMAR, Linear Interpolation Metal Artifact Reduction (LIMAR) and Convolutional-Neural-Network-based Metal Artifact Reduction (CNNMAR).

DOI: 10.54254/2753-8818/2026.33015

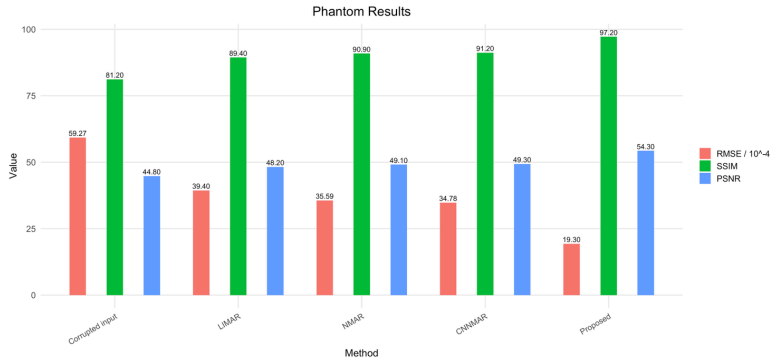


Figure 11. Quantitative results of the phantom study [10]

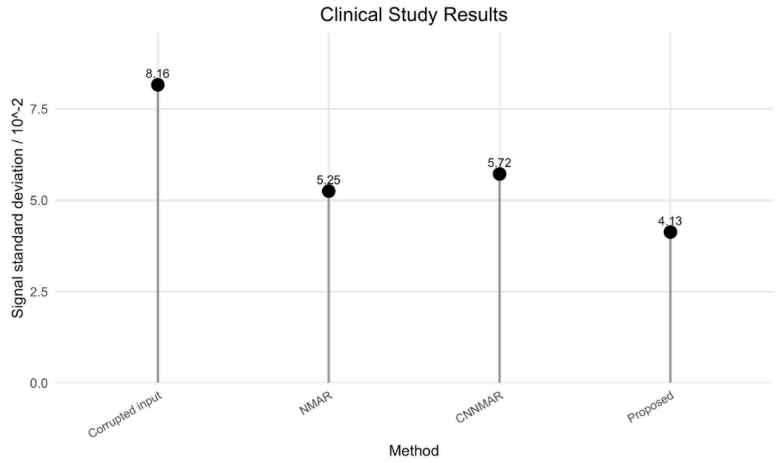


Figure 12. Standard deviation calculated over flat soft tissue ROI [10]

Quantitative results from the phantom study (Figure 11) indicated that the hybrid approach achieved lower RMSE than all comparators, and soft tissue standard deviation analysis (Figure 12) demonstrated superior noise suppression and streak reduction. In addition, their method successfully preserved tissue structures with little harm in the clinical image.

Notwithstanding such a great progress their method has made, some problems remain unsolved. First, one full LDMNMAR takes 202 s which might cause trouble in practical occasions. Second, the patients in their clinical study were not able to take off their metals like restorations and implants, which led to no clean image served as the ground truth. This weakens the practical value and verification for their clinical evaluation is needed. Third, although the secondary artifacts reduction was alleged to lessen residual artifacts, intrinsic normal details was found lost [10].

3.3.2. Conditional diffusion model for exomass-related artifacts

The exomass artifacts, which occur when part of the object exceeds the boundaries of FOV, have always been tricky tasks in oral medicine because dental CBCTs often adopt relatively smaller FOV and metal materials are frequently present. Also, the usual MAR algorithms are not specialized in dealing with this sort of artifacts so that streaks often exist near the image edges and noise level is elevated. Therefore, Oliveira et al. established a deep-learning model called Denoising Diffusion Probabilistic Model (DDPM) to dedicatedly mitigate exomass artifacts. They scanned five porcine

DOI: 10.54254/2753-8818/2026.33015

mandibles using 4 CBCT units and change the implants material and amounts for each scan. The scans without any implants were treated as the ground truth.

To substantiate the effectiveness of the proposed method, Oliveira et al. divided the evaluation into 2 parts, qualitative and quantitative. For the qualitative evaluation, the radiologists scored different images with the scale from 1 to 5 according to both hard tissue visualization and general image quality. They reported that the DDPM-corrected images beat the original ones in both aspects and all got high scores around 4. Moreover, the stability of image quality in DDPM groups was higher, which meant that DDPM rendered the original images less susceptible to varied implants. To figure out how rigorous the radiologists' ratings were, a Kappa test was performed, and the results showed that the intra-examiner reliability was 0.94 and inter-examiner reliability was 0.79. Both reached the criterion. For quantitative evaluation, contrast-to-noise ratio (CNR) was used as the only metric. In the 36 groups across different CBCT unit, materials and implant numbers, the DL-corrected images gained more CNR ranging from 4.2 to 32.1, with only one exception in which CNR was diminished by 1.4 under the condition where two titanium implants were used in the ProMax 3D Max CBCT. The significance threshold for determining whether the CNR decline was due to chance was $P < 0.05$, indicating statistical significance.

The major drawback of DDPM is inconsistency of grayscale across slices because this model was developed and trained via individual axial images rather than 3D data. Besides, the resolution will become lower if using DDPM because the image size must be modulated for this model. The deeper reason is related to the GPU [11].

3.4. Dual-energy CBCT and virtual monoenergetic imaging

Because metal artifact reduction remains challenging in dental CBCT, especially when conventional post-processing methods provide only limited improvement, energy-based imaging strategies have become an important direction of investigation. Among them, dual-energy CT combined with virtual monoenergetic imaging has demonstrated clear potential for reducing metal artifacts by alleviating photon starvation. However, dual-energy CT is still rarely employed in dental practices because of its high hardware cost. To incorporate the advantage of DE CT in oral medicine with lower cost, Li et al. self-made a carbon nanotube (CNT) x-ray tube with two focal spots to substitute for the original one on a normal dental CBCT but kept the FPD unchanged, then mounted two different filters to obtain two levels of energy. Two head phantoms embedded with steel beads were used as objects and a single-energy dental CBCT served as the comparator.

Qualitative results suggested that the VMI-processed image with energy of 120 and 140 keV manifested much less artifacts than the common dental CBCT image. Moreover, for the dual energy realized by filters, the high energy level reduced more artifacts but produced more noise instead. For quantitative metrics, Metal Artifact Index (MAI) exhibit an inverse relationship with increasing energy and achieved lowest at 150 keV which was the upper end of the VMI energy range. And the 150 keV synthesized energy also elevated the average HU in the dark band region from -1150 to -950 HU, indicating that they were not that black before. In terms of the CNR, it reached the top at 80 keV then dropped as energy was synthesized higher. Therefore, a trade-off appeared between noise and artifacts reduction. Higher energy above 80 keV mitigated artifacts more but escalated noise levels. At last, to test the feasibility of the self-made DE CBCT, the total scan time was estimated to be approximately 18.8 s which was roughly equivalent with regular dental CBCT.

One big limitation of this acquisition and post-processing modality is that the material decomposition method has to be included instead of fixing the projection data which was acknowledged to be more efficacious by authors. Besides, another limitation was that the newly

DOI: 10.54254/2753-8818/2026.33015

developed two-focal-spot design caused stronger blurring, measuring 0.41 mm and 1.2 mm for the low- and high-energy settings, respectively, in this experiment. At last, the filters which separate energies are of so limited strength that only 20 keV can be split [12].

Similar to Li et al.'s artifact-mitigation strategy, Jayakody et al. also discovered the limited use of dual-energy CBCT in dentistry and its potential advantages when combined with VMI. What differentiated from Li et al. was that Jayakody et al. integrated dual-energy, projection-domain material decomposition, VMI and vendor MAR together as a hybrid modality. Furthermore, they did not reconfigure any hardware but scanned the same objects with two different X-ray energy with the intention of implementing the dual-energy exposure. Phantoms before and after being inserted any restorative or prosthetic materials were scanned to provide reference ROI and comparisons across different material kinds. The subsequent workflow of the proposed method is shown in Figure 13.

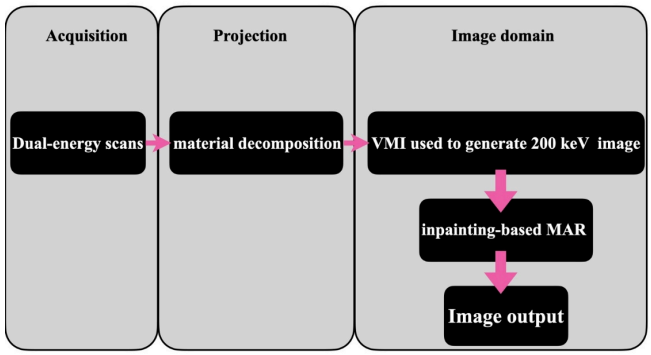


Figure 13. The workflow of the hybrid proposed method [13]

Comparators of this method included regular single-energy 100kV reconstruction as the baseline, VMI, vendor's classic MAR and VMI + MAR. At last, artifact scores were calculated by subtracting the pixel values in the reference ROI from those in the artifact-affected ROIs. Qualitative evaluation showed that, using the routine 100 kV image as the baseline, both VMI and MAR reduced artifacts, but the combined approach achieved the highest efficacy because VMI alone left many residual artifacts, whereas MAR alone introduced additional streaks. Quantitative findings demonstrated that in all six materials, the 4 methods could be ranked from best to worst as: VMI + MAR, VMI, inpainting MAR and 100 kV. Overall, the proposed method performed best in the comparative evaluation.

Notwithstanding the huge success it has made, one fatal flaw for this acquisition modality exists: the scan of two energy levels has to be separated with a temporal interval when motions might occur. This will cause anatomy structures in two images cannot be matched therefore following steps will also be futile. Moreover, only water and iron were used as the basis for material decomposition but they are not able to represent such a complex family of dental materials sufficiently [13].

3.5. Cross-study synthesis

Across the included studies, several common patterns can be identified. First, the current evidence base still relies mainly on phantom, ex vivo, and cadaver models, whereas purely clinical validation remains limited. Although some studies incorporated patient images, most methods have not yet been tested under sufficiently broad real-world clinical conditions. This indicates that current findings are promising but still transitional in terms of clinical translation.

DOI: 10.54254/2753-8818/2026.33015

Second, most artifact reduction strategies were concentrated in the projection domain or combined multiple stages of the imaging chain, whereas reconstruction-only approaches were less common. This trend suggests that correcting inconsistencies before or alongside reconstruction is still considered more effective than relying on a single downstream step. In addition, most studies focused on metal-related artifacts, while relatively few specifically targeted scatter or noise alone.

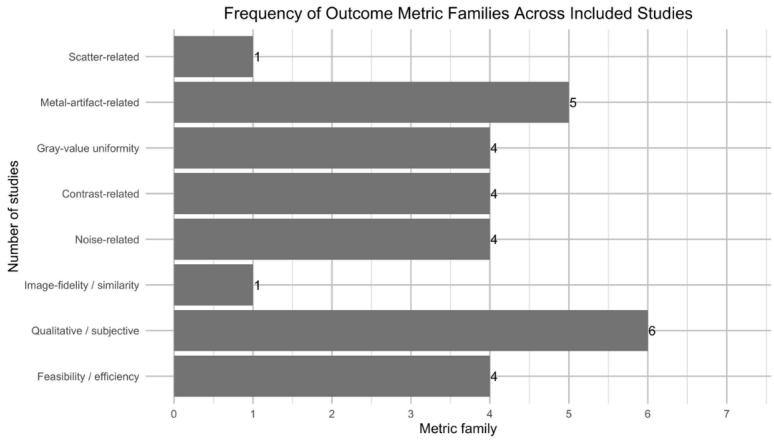


Figure 14. Frequency of metrics reported across the included studies

Picture credit : original

The distribution of evaluation metrics across the included studies is summarized in Figure 14. Commonly used endpoints included HU uniformity, contrast-to-noise ratio, artifact scores, and qualitative assessment, but direct comparison across studies remained difficult because of differences in experimental design and evaluation criteria. This lack of standardization limits robust cross-method comparison and further highlights the need for more clinically relevant and consistent evaluation frameworks.

4. Future directions

Concerning the newest imaging technologies, photon-counting CT (PCCT) has been praised for high spatial resolution, dose efficiency, and spectral information, which are also the advantages pursued by dual-energy approaches in dental CBCT research. PCCT has an acquisition-based potential for mitigating metal artifacts at the acquisition stage, particularly when combined with VMI and iMAR. However, it is rarely employed in clinical dental imaging owing to the lack of software dedicated for dentistry and agreeing protocols, as well as high cost. At present, the viability of PCCT requires more and constant clinical statistics as support [14].

5. Conclusion

Because of the larger FPD, cone-beam geometry, low dose adopted by dental CBCT, scatter, beam-hardening and photon starvation are more substantial. In addition to the exacerbation of these effects caused by metals, which are especially common in dentistry, more artifacts appear and obstruct diagnosis. Researchers have developed many methods to mitigate artifacts across acquisition, projection-domain, reconstruction and image-domain. Among them, correction of projections before reconstruction has been mostly used and mitigation strategies are gradually progressing from single-step processing toward more multi-stage and complementary technical modalities. In addition,

DOI: 10.54254/2753-8818/2026.33015

algorithms or deep-learning models are much easier to deploy in practice than hardware-based method such as ASG.

Gaps remain in current research. First, limited experimental objects such as phantoms, ex vivo specimens, and cadavers cannot substitute for real patients. The currently available evidence in clinical scenarios is still neither robust nor sufficient. Second, the outcome assessment needs to be more explicit via using more quantitative metrics rather than qualitative evaluations. Third, cross-method comparison is challenging to undertake because metrics used for assessing image quality are heterogeneous across contrast, noise and artifacts index. However, spatial resolution and restoration of fine anatomy details, which are often prioritized by radiologists, are rarely mentioned.

Fusion of methods across different imaging steps as well as both hardware and software are likely to be a common feature in future artifacts reduction methods. More solid clinical validation, cross-device testing, and a more unified evaluation framework need to be incorporated in future researches. Moreover, emerging technologies like spectral CT, including dual-energy CT and PCCT, material decomposition and VMI will be applied in dental CBCT as more substantial clinical validations are conducted.

References

[1] Zhao, W., Vernekohl, D., Zhu, J., Wang, L., and Xing, L. (2016) A model-based scatter artifacts correction for cone beam CT. Medical Physics, 43(4), 1736–1753.
[2] Sawicki, P., Zawadzki, P. J., and Regulski, P. (2022) The impact of cone-beam computed tomography exposure parameters on peri-implant artifacts: A literature review. Cureus, 14(3), e23035.
[3] Zeng, G. L. (2022) Photon starvation artifact reduction by shift-variant processing. IEEE Access : Practical Innovations, Open Solutions, 10, 13633–13649.
[4] Parsa, A., Ibrahim, N., Hassan, B., Syriopoulos, K., and van der Stelt, P. (2014) Assessment of metal artefact reduction around dental titanium implants in cone beam CT. Dentomaxillofacial Radiology, 43(7), 20140019.
[5] Li, B., Somerkivi, V., Bayat, F., Huynh, C., and Altunbas, C. (2025) Effect of a prototype 2-dimensional antiscatter grid on image quality obtained with a dental cone-beam computed tomography scanner. Imaging Science in Dentistry, 55(1), 37–47.
[6] Sabounchi, R., Pyakurel, U., Bayat, F., Eldib, M., Ozus, B., Crockett, B., and Altunbas, C. (2025) Improving Hounsfield unit accuracy in dental CBCT through the integration of 2D anti-scatter grid. Oral Radiology, 41(4), 485–497.
[7] Hegazy, M. A. A., Cho, M. H., Cho, M. H., and Lee, S. Y. (2023) Metal artifact reduction in dental CBCT images using direct sinogram correction combined with metal path-length weighting. Sensors, 23(3), 1288.
[8] Shi, L., Bennett, N. R., Shiroma, A., Sun, M., Zhang, J., Colbeth, R., Star-Lack, J., Lu, M., and Wang, A. S. (2021) Single-pass metal artifact reduction using a dual-layer flat panel detector. Medical Physics, 48(10), 6482–6496.
[9] Ramage, A., Lopez Gutierrez, B., Fischer, K., Sekula, M., Santaella, G. M., Scarfe, W., Brasil, D. M., and de Oliveira-Santos, C. (2023) Filtered back projection vs. iterative reconstruction for CBCT: Effects on image noise and processing time. Dento Maxillo Facial Radiology, 52(8), 20230109.
[10] Choi, D.-I., Yun, S., Hyun, S., and Cho, S. (2025) Metal artifact reduction algorithm with conditional latent diffusion model for dental cone-beam CT. Journal of Applied Clinical Medical Physics, 26(11), e70317.
[11] Oliveira, M. L., Schaub, S., Dagassan-Berndt, D., Bieder, F., Cattin, P. C., and Bornstein, M. M. (2025) Development and evaluation of a deep learning model to reduce exomass-related metal artefacts in cone-beam CT: An ex vivo study using porcine mandibles. Dento Maxillo Facial Radiology, 54(2), 109–117.
[12] Li, B., Spronk, D., Luo, Y., Puett, C., Inscoe, C. R., Tyndall, D. A., Lee, Y. Z., Lu, J., and Zhou, O. (2022) Feasibility of dual-energy CBCT by spectral filtration of a dual-focus CNT x-ray source. PLoS ONE, 17(2), e0262713.
[13] Jayakody, D., Agrawal, H., Räinä, E., Sipola, A., Näpänkangas, R., Ylisiurua, S., Nieminen, M. T., and Brix, M. (2025) A hybrid approach combining dual-energy and inpainting methods for metal artifact reduction in dentomaxillofacial CBCT: A proof-of-concept phantom study. Annals of Biomedical Engineering, 53(10), 2638–2647.
[14] Zanon, C., Pepe, A., Cademartiri, F., Bini, C., Maffei, E., Quaia, E., Stellini, E., and Di Fiore, A. (2024) Potential benefits of photon-counting CT in dental imaging: A narrative review. Journal of Clinical Medicine, 13(8), 2436.